Tetrahedron 65 (2009) 305–311

Contents lists available at ScienceDirect

Tetrahedron

journal homepage: www.elsevier.com/locate/tet

Heterogeneous chiral Mn(III) salen catalysts for the epoxidation of unfunctionalized olefins immobilized on mesoporous materials with different pore sizes

Kai Yu, Zhicheng Gu, Runan Ji, Lan-Lan Lou, Shuangxi Liu *

Institute of New Catalytic Materials Science, College of Chemistry, Nankai University, Tianjin 300071, China

ARTICLE INFO

Article history:
Received 3 June 2008
Received in revised form 13 October 2008
Accepted 17 October 2008
Available online 1 November 2008

Keywords:
Chiral Mn(III) salen complex
Mesoporous materials
Fine-tuning of pore size
Immobilization
Asymmetric epoxidation

ABSTRACT

Two chiral Mn(III) salen complexes were immobilized onto a series of mesoporous MCM-41 and MCM-48 materials with different pore sizes and the as-synthesized catalysts were active and enantioselective for the asymmetric epoxidation of styrene and indene. The results of XRD, FTIR, DR UV–vis, and N_2 sorption showed that the chiral Mn(III) salen complexes were anchored in the channels of mesoporous materials. The influence of organic silicane dosage on the catalytic performance was studied and the optimum dosage of organic silicane for preparing heterogeneous catalysts was determined. Furthermore, the effect of the fine-tuning of pore size on the performance of heterogeneous catalysts was discussed. In general, larger pore size of the supports could lead to higher conversions and the compatible pore size with substrate may be responsible for the improved enantiomeric excess (ee) values.

1. Introduction

Chiral Mn(III) salen complexes have proven activity and enantioselectivity for the asymmetric epoxidation of unfunctionalized olefins,[1,2] which are highly significant in the pharmaceutical and agrochemical fields to synthesize chiral building blocks that could be transformed into other useful chiral compounds through regioselective ring-opening reactions.[3] However, the catalyst always suffers from separation and recycling problems in homogeneous system. Consequently, the heterogenization of chiral Mn(III) salen complexes within inorganic matrixes has received great attention[4–13] over the last decade. The heterogeneous catalysts could be easily separated from the reaction system and simply recycled several times, moreover, the immobilization of chiral Mn(III) salen complexes could effectively decrease the formation of inactive dimeric μ-oxo Mn(IV) species.[14]

The mesoporous siliceous materials have large surface areas, controllable pore sizes of 2–50 nm, and abundant silanol groups on the surface, allowing ready material diffusion and easily organically functionalized and grafted to catalytic active species, and thus were widely applied in the immobilization of chiral Mn(III) salen complexes.[3,15–23] Recently, the influence of pore size on the catalytic performance of mesoporous material-supported chiral Mn(III) salen complex has been reported. Zhang et al.[3,15] immobilized the chiral Mn(III) salen complexes into the nanopores of mesoporous supports MCM-41(1.6 and 2.7 nm), SBA-15 (7.6 nm), and activated silica (9.7 nm) with different pore sizes and the influence of pore size on the catalytic performance was studied. Kureshy et al.[16,17] supported the chiral Mn(III) salen complex onto the mesoporous materials MCM-41 and SBA-15, and found that the SBA-15-based catalyst, with a larger pore diameter, was more active than MCM-41-supported catalyst. Similarly, Thomas et al.[24] and Raja et al.[25] also studied the influence of pore size on catalytic performance for other heterogeneous asymmetric reactions.

It is generally believed that the pore size of parent supports could influence the activity and enantioselectivity of the heterogeneous chiral Mn(III) salen catalysts. However, the effect of the fine-tuning of pore size on the catalytic performance of mesoporous material-supported chiral Mn(III) salen complex has seldom been systematically investigated for the heterogeneous asymmetric epoxidation. In this work, the chiral Mn(III) salen complexes were immobilized onto a series of mesoporous MCM-41 and MCM-48 materials, which possess the pore sizes varied on the angstrom length-scale. The as-synthesized catalysts were evaluated in the epoxidation of styrene and indene. The effects of organic silicane dosage and the fine-tuning of pore size on the performance of heterogeneous catalysts were studied.

* Corresponding author. Tel./fax: +86 22 23509005.
E-mail address: sxliu@nankai.edu.cn (S. Liu).

0040-4020/$ – see front matter © 2008 Elsevier Ltd. All rights reserved.
doi:10.1016/j.tet.2008.10.051

2. Experimental

2.1. Materials

3-Mercaptopropyltrimethoxysilane, *cis*/*trans*-1,2-diaminocyclohexane, and 2-*tert*-butylphenol were supplied by Alfa Aesar. *m*-Chloroperbenzoic acid (*m*-CPBA) was purchased from Acros Organics. *N*-Methylmorpholine-*N*-oxide (NMO) was provided by Aldrich. Indene was purchased from Fluka. Alkyltrimethylammonium bromides $C_nH_{2n+1}(CH_3)_3$–NBr (C_nTAB for brevity, n=12, 14, 16, 18; AR) were obtained from Jintan Huadong Chemical Research Institute in Jiangsu. (1*R*,2*R*)-(+)-1,2-Diphenylethylenediamine (>99% ee) was provided by Likai Chiral Tech. Co. Ltd. in Chengdu. (1*R*,2*R*)-(−)-1,2-Diaminocyclohexane was resolved from the technical grade isomers mixture in >99% ee by the reported procedure.[26] Tetraethyl orthosilicate (TEOS), 2,2′-azobis(2-methylpropionitrile) (AIBN), and styrene were provided by Jiangtian Co. Ltd. in Tianjin. Racemic epoxides were synthesized by the epoxidation of corresponding olefins with *m*-CPBA in $CHCl_3$ at 273 K[27] and detected by gas chromatography (GC). All of the solvents used in the present study were purified before use.

2.2. Characterization

Powder X-ray diffraction (XRD) patterns were performed on an R/max-2500 diffractometer with Cu Kα radiation at 40 kV and 100 mA in a scan range of $1.5°<2\theta<10°$. FTIR spectra were carried out on KBr pellets in a BRUKER VECTOR 22 spectrometer. Diffuse-reflectance UV–vis (DR UV–vis) spectra were obtained on a Shimadzu UV-2550 UV–vis spectrophotometer in the range of 220–800 nm. N_2 adsorption–desorption analysis was carried out at 77 K on a Micromeritics TriStar 3000 apparatus. The analytical data were processed by the BET equation for surface areas and by the BJH model for pore size distributions. Elemental analysis was performed on a Perkin–Elmer 240C analyzer. ^{1}H and ^{13}C{^{1}H} NMR spectra were recorded at 300 and 75 MHz, respectively, using a Varian Mercury Vx-300 spectrometer. The content of Mn in the heterogeneous catalysts was determined by an ICP-9000 (N+M) spectrometer (TJA Co.), after calcination and solubilization of the samples with hydrogen fluoride and aqua regia. The products of epoxidation reaction were determined by GC with a chiral β-cyclodextrin capillary column (RESTEK RT-BetaDEXse, 30 m×0.25 mm×0.25 μm), using a Rock GC7800 gas chromatograph equipped with a flame ionization detector. Ultrapure nitrogen was used as the carrier gas and the column temperature was programmed in the range of 333–423 K. For each of the epoxidation reactions, the conversion and ee value were determined by averaging the values from two parallel measurements, of which the results should not differ by more than 0.5%, otherwise additional measurements on the same sample need to be done.

2.3. Synthesis of siliceous mesoporous materials

A series of highly ordered siliceous mesoporous materials MCM-41 and MCM-48 with different pore sizes were synthesized according to the literature method,[28–30] using the alkylammonium salts C_nTAB (n=12, 14, 16, 18) with different alkyl chain lengths as templates and TEOS as silica source.

2.3.1. Synthesis of MCM-41 with different pore sizes

The highly ordered hexagonal siliceous MCM-41 materials with different pore sizes were synthesized using a gel (molar) composition of $1TEOS/0.12C_nTAB/8NH_4OH/114H_2O$. In a typical synthesis, the template of C_nTAB was dissolved in warm deionized water. To this solution, ammonia and TEOS were added orderly under vigorous stirring. After stirring at room temperature for 0.5 h, the resulting gel was allowed to crystallize at 383 K for 52 h in a Teflon-lined autoclave. The solid product was filtered, washed with deionized water, dried at room temperature, and calcined at 823 K in air for 6 h to remove the template. According to the difference in the alkyl chain length of the template, the as-synthesized materials were marked as *n*MCM-41 (n=12, 14, 16, 18).

2.3.2. Synthesis of MCM-48 with different pore sizes

The mesoporous materials MCM-48 with different pore sizes were synthesized according to the procedures as follows. When C_nTAB (n=14,16) was used as template, C_nTAB was dissolved in warm deionized water, and to this solution the required quantity of TEOS and the aqueous solution of NaOH were added in sequence under vigorous stirring. After stirring for 2 h at room temperature, a gel with a molar composition of $1TEOS/0.46C_nTAB/0.41NaOH/52.95H_2O$ was obtained. The resulting gel was allowed to crystallize at 383 K for 72 h in a Teflon-lined autoclave. When C_nTAB (n=12) was used as template, the molar composition of the gel was $1TEOS/1.10C_nTAB/0.46NaOH/112H_2O$, and the gel was crystallized at 393 K for 168 h. Then, the solid product was filtered, washed with deionized water, and dried in air at room temperature overnight. The template was removed by calcination at 823 K in air for 6 h. According to the difference in the alkyl chain length of the template, the as-synthesized materials were marked as *n*MCM-48 (n=12, 14, 16).

2.4. Synthesis of the homogeneous chiral Mn(III) salen complex

The chiral Mn(III) salen complexes **1** and **2** were obtained through the synthesis sequence given in Scheme 1 according to the literature.[31]

2.4.1. Synthesis of 3-tert-butyl-2-hydroxy-5-vinylbenzaldehyde (*D*)

3-*tert*-Butyl-2-hydroxybenzaldehyde (**A**) was synthesized from 2-*tert*-butylphenol as described previously.[32] Compound **A** (27.0 g, 0.15 mol), paraformaldehyde (10.0 g, 0.33 mol), and tetrabutylammonium bromide (4.7 g, 14.6 mmol) were stirred in concentrated hydrochloric acid (110 mL) at 313 K for 3 days.[33] The reaction mixture was extracted with diethyl ether (3×150 mL), and the organic phase was washed with 5% $NaHCO_3$ (2×100 mL), brine (2×100 mL), and dried over $MgSO_4$. Evaporation of the solvent under vacuum afforded 3-*tert*-butyl-5-chloromethyl-2-hydroxybenzaldehyde (**B**) as a yellow crystalline solid (34.0 g, 99% yield). ^{1}H NMR ($CDCl_3$, 300 MHz): δ (ppm) 1.43 (s, 9H), 4.59 (s, 2H), 7.44 (d, J=1.8 Hz, 1H), 7.53 (d, J=1.8 Hz, 1H), 9.87 (s, 1H), 11.87 (s, 1H).

A mixture of compound **B** (15.9 g, 0.070 mol) and triphenylphosphine (18.3 g, 0.070 mol) was refluxed in cyclohexane (150 mL) for 1 h. After cooling the solution to room temperature, the product was filtered, washed with diethyl ether, and dried under vacuum. Then, 3-*tert*-butyl-5-formyl-4-hydroxybenzyl(triphenylphosphonium) chloride (**C**) (30.9 g, 90% yield) was obtained as a white powder. ^{1}H NMR ($CDCl_3$, 300 MHz): δ (ppm) 1.13 (s, 9H), 5.66 (d, J=13.8 Hz, 2H), 7.32 (d, J=1.8 Hz, 2H), 7.62–7.86 (m, 15H), 9.70 (s, 1H), 11.82 (s, 1H).

Compound **C** (24.6 g, 0.050 mol) was stirred in 170 mL of 40% aqueous formaldehyde, and an aqueous solution of 12.5 N NaOH (55 mL) was added, keeping the reaction temperature below 313 K. After stirring at room temperature for 2 h, the mixture was cooled with ice and neutralized with 6 N HCl. At pH ≈ 7, the aqueous phase was extracted with cyclohexane. Evaporation of the solvent afforded a semisolid that was purified by flash chromatography (dichloromethane). After distilled under vacuum (380 K, 0.1 mmHg), 3-*tert*-butyl-2-hydroxy-5-vinylbenzaldehyde (**D**) (5.87 g, 57% yield) was obtained as light yellow crystals. ^{1}H NMR ($CDCl_3$, 300 MHz): δ (ppm) 1.43 (s, 9H), 5.21 (d, J=11.1 Hz, 1H), 5.66 (d, J=17.7 Hz, 1H), 6.68 (dd, J=17.4, 10.8 Hz, 1H), 7.41 (d, J=2.1 Hz, 1H), 7.61 (d, J=2.1 Hz, 1H), 9.89 (s, 1H), 11.79 (s, 1H).

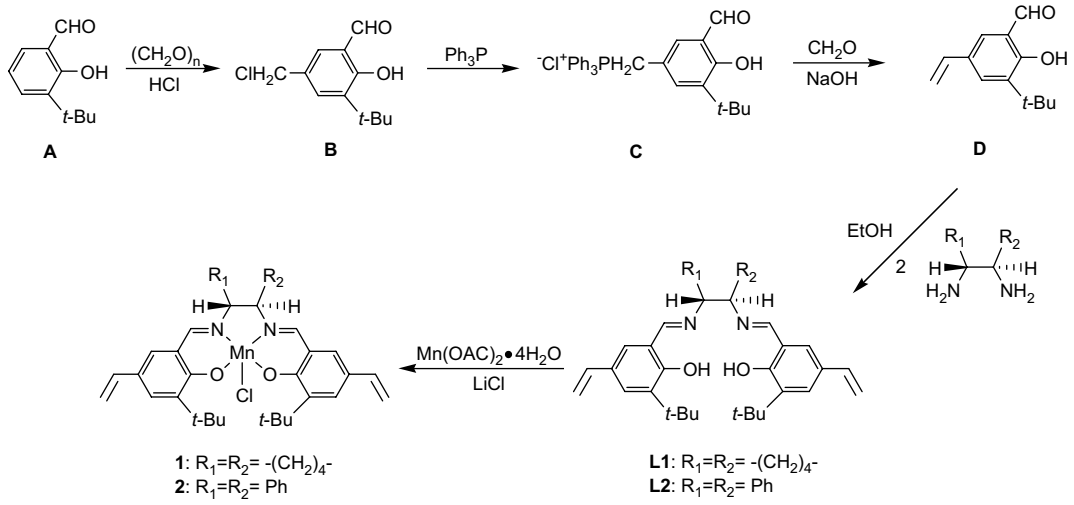

Scheme 1. The synthesis process of chiral Mn(III) salen complexes **1** and **2**.

*2.4.2. Synthesis of the chiral salen ligand **L1***

Compound **D** (1.23 g, 6.00 mmol) and (1*R*,2*R*)-(−)-1,2-diaminocyclohexane (0.34 g, 3.00 mmol) were dissolved in 15 mL of hot ethanol, and the resulting solution was refluxed for 1 h. After partial removal of the solvent, the solution was kept at 273–277 K for 12 h, and the product **L1** was collected by filtration as deep yellow crystals (1.33 g, 91%). ^{1}H NMR ($CDCl_3$, 300 MHz): δ (ppm) 1.41 (s, 18H), 1.45–1.97 (m, 8H), 3.31–3.34 (m, 2H), 5.04 (d, J=10.8 Hz, 2H), 5.49 (d, J=17.4 Hz, 2H), 6.55 (dd, J=17.4, 11.1 Hz, 2H), 7.02 (d, J=2.1 Hz, 2H), 7.31 (d, J=2.1 Hz, 2H), 8.28 (s, 2H), 13.96 (s, 2H). ^{13}C{^{1}H} NMR (75 MHz in $CDCl_3$): δ (ppm) 24.2, 29.3, 32.9, 34.8, 72.3, 110.8, 118.4, 127.2, 127.5, 136.3, 137.1, 159.8, 165.3.

*2.4.3. Synthesis of the chiral salen ligand **L2***

Compound **D** (613 mg, 3.00 mmol) and 319 mg (1.50 mmol) of (1*R*,2*R*)-(+)-1,2-diphenylethylenediamine were refluxed in 10 mL of ethanol. Following the same procedure described above for the preparation of ligand **L1**, 842 mg of ligand **L2** (96% yield) was obtained as deep yellow crystals. ^{1}H NMR ($CDCl_3$, 300 MHz): δ (ppm) 1.42 (s, 18H), 4.72 (s, 2H), 5.05 (d, J=10.8 Hz, 2H), 5.49 (d, J=17.4 Hz, 2H), 6.55 (dd, J=17.7, 10.8 Hz, 2H), 7.02 (d, J=2.1 Hz, 2H), 7.18–7.26 (m, 10H), 7.33 (d, J=2.1 Hz, 2H), 8.35 (s, 2H), 13.84 (s, 2H). ^{13}C{^{1}H} NMR (75 MHz in $CDCl_3$): δ (ppm) 29.3, 34.8, 80.0, 110.9, 118.3, 127.5, 127.6, 127.8, 128.0, 136.3, 137.3, 139.3, 160.2, 166.9.

*2.4.4. Synthesis of the chiral Mn(III) salen complexes **1** and **2***

The chiral ligand **L1** (or **L2**) (2.0 mmol) and $Mn(OAc)_2 \cdot 4H_2O$ (1.24 g, 5.0 mmol) were refluxed in ethanol (30 mL) for 1 h. Then, LiCl (0.6 g, 15 mmol) was added, and the mixture was refluxed for an additional 1 h under exposure to the air. The solvent was completely removed under vacuum and the residue was dissolved in dichloromethane (100 mL). The organic phase was washed with deionized water (3×25 mL), brine (2×20 mL), and then dried over $MgSO_4$. After evaporation of the solvent, the residue was recrystallized from dichloromethane/hexane to give **1** (or **2**) as a brown solid. Mn(III) salen complex **1**: FTIR (KBr): 3077, 2956, 2862, 1611, 1538, 1456, 1436, 1386, 1340, 1310, 1265, 1233, 1202, 1165, 1097, 1029, 987, 898, 825, 793, 772, 557 cm^{-1}; DR UV–vis: 284, 320, 366, 448, 532 nm. Mn(III) salen complex **2**: FTIR (KBr): 3077, 2956, 2862, 1606, 1538, 1456, 1436, 1386, 1340, 1310, 1270, 1239, 1207, 1165, 987, 882, 851, 814, 783, 725, 699, 568 cm^{-1}; DR UV–vis: 284, 328, 366, 456, 550 nm.

2.5. Heterogenization of chiral Mn(III) salen complexes 1 and 2

The synthesis process is shown in Scheme 2. The calcined siliceous mesoporous support (1.0 g) and the required quantity of 3-mercaptopropyltrimethoxysilane were stirred in 80 mL of anhydrous toluene under refluxing for 8 h. The resulting solid was filtered, washed with ethanol, and dried at 323 K under vacuum for 12 h. The dried mercaptopropylsilyl-functionalized mesoporous material (1.0 g), the chiral Mn(III) salen complex **1** or **2** (0.20 mmol), and AIBN (0.015 g, 0.10 mmol) were refluxed under nitrogen in 30 mL of oxygen-free chloroform for 12 h. The samples were collected by filtration, washed with ethanol, and Soxhlet-extracted with dichloromethane for 24 h. According to the difference of the supports and the chiral Mn(III) salen complexes, the heterogeneous catalysts were marked as ***n*M41-1**(or ***n*M41-2**) (n=12, 14, 16, 18) and ***n*M48-1** (or ***n*M48-2**) (n=12, 14, 16).

2.6. Asymmetric epoxidation of unfunctionalized olefins

The epoxidation reactions were carried out using the catalysts (0.015 mmol) with styrene and indene as substrates (1 mmol) and

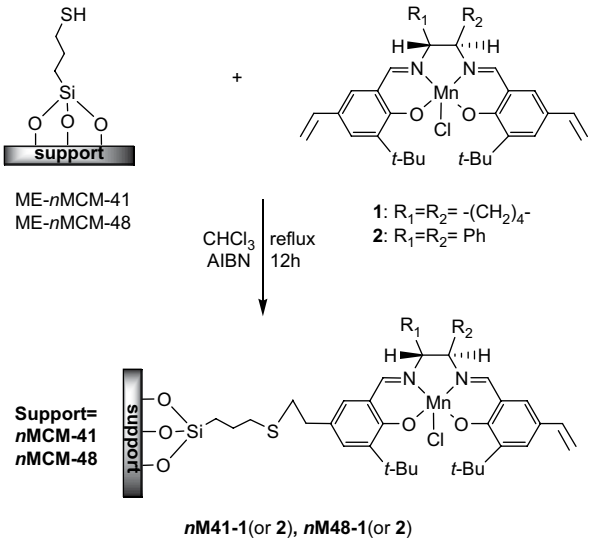

Scheme 2. Preparation of the heterogeneous chiral Mn(III) salen catalysts.

Table 1
The structure parameters of mesoporous materials *n*MCM-41 and *n*MCM-48

Sample	S_{BET} ($m^2\,g^{-1}$)	Pore volume ($cm^3\,g^{-1}$)	Pore diameter (Å)
18MCM-41	1112	1.11	31.7
16MCM-41	941	0.82	27.9
14MCM-41	841	0.71	21.9
12MCM-41	873	0.59	18.9
16MCM-48	1200	1.11	26.0
14MCM-48	1201	0.80	23.2
12MCM-48	1257	0.82	18.6

m-CPBA (2 mmol) as an oxidant in 10 mL of dichloromethane containing toluene (40 μL) as an internal standard and NMO (5 mmol) as an axial base at 273 K. Once the reaction was completed, the supported catalysts were separated by filtration, and the filtrate was washed with 1 N NaOH (10 mL) and brine (10 mL), then dried over $MgSO_4$. The conversion and ee values were determined by GC, with toluene as an internal standard. For the heterogeneous catalysis system, the filtrate was detected by ICP-AES, and no obvious Mn leaching (<0.5%) was found.

3. Results and discussion

3.1. Characterization of the supports

The mesoporous materials *n*MCM-41 and *n*MCM-48 were characterized by N_2 sorption. The BET surface area, pore volume, and pore diameter of all the parent supports are given in Table 1. The obtained mesoporous materials *n*MCM-41 and *n*MCM-48 have large BET surface area and pore volume. Moreover, with the decrease in alkyl chain length of the templates, the pore diameter of the mesoporous materials regularly decreased on the angstrom length-scale.

3.2. Characterization of the heterogeneous catalysts

The powder XRD patterns of the calcined supports (16MCM-41 and 16MCM-48), the mercaptopropylsilyl-functionalized supports (ME-16MCM-41 and ME-16MCM-48), and the heterogeneous catalysts (**16M41-1**, **16M41-2**, **16M48-1** and **16M48-2**) are shown in Figure 1. After modification by 3-mercaptopropyltrimethoxysilane and immobilization of Mn(III) salen complexes, the intensities of all peaks decreased. However, the well-resolved reflections (110) and (200) for 16MCM-41-supported catalysts and reflection (220) for 16MCM-48-supported catalysts indicated that the mesoporous structure of heterogeneous catalysts still kept good periodicity.

The FTIR spectra of chiral Mn(III) salen complexes (**1** and **2**) and the heterogeneous catalysts (**16M48-1** and **16M48-2**) are shown in Figure 2. The bands near 3000 cm^{-1} were due to C–H stretching vibrations of alkyl groups, and the IR bands near 1540 cm^{-1} were attributed to the stretching vibrations of azomethine groups (H–C═N). The deformation vibrations of C–H bond in alkyl groups appeared in the range of 1340–1456 cm^{-1}. The characteristic IR bands of the chiral Mn(III) salen complexes could be also observed in the FTIR spectra of heterogeneous catalysts. The results of FTIR characterization confirmed the successful immobilization of chiral Mn(III) salen complex.

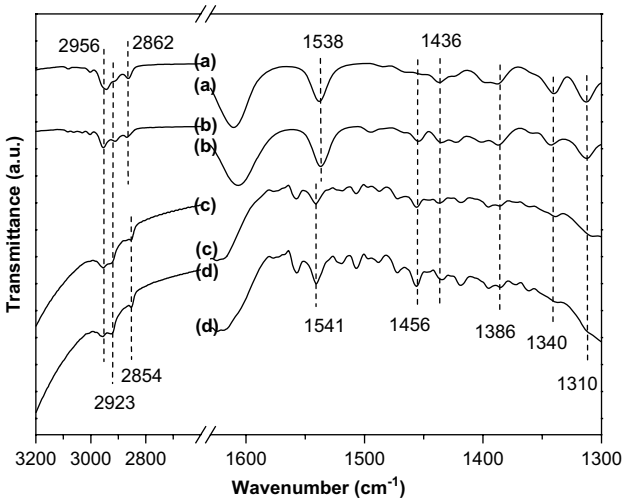

Figure 2. FTIR spectra of (a) Mn(III) salen complex **1**, (b) the heterogeneous catalyst **16M48-1**, (c) Mn(III) salen complex **2**, and (d) the heterogeneous catalyst **16M48-2**.

The diffuse-reflectance UV–vis spectra of chiral Mn(III) salen complexes (**1** and **2**) and the heterogeneous catalysts (**16M48-1** and **16M48-2**) are shown in Figure 3. In the spectrum of chiral Mn(III) salen complexes, the bands at 284, 320, 328, and 366 nm were due to the charge transfer transition of salen ligand, the bands at 448 and 456 nm could be attributed to ligand-to-metal charge transfer transition, and the bands at 532 and 550 nm may be assigned to the d–d transition of Mn(III) salen complexes. The spectra of heterogeneous catalysts **16M48-1** and **16M48-2** showed features similar to those of homogeneous catalysts **1** and **2**. However, after immobilization of Mn(III) salen complex on mesoporous materials, the bands at 284 and 448 nm shifted to 268 and 434 nm for **16M48-1**, and the bands at 284 and 456 nm shifted to 271 and 440 nm for **16M48-2**. The blue shift indicated the presence of interaction between Mn(III) salen complex and the support, and further confirmed the immobilization of chiral Mn(III) salen complexes on the supports.

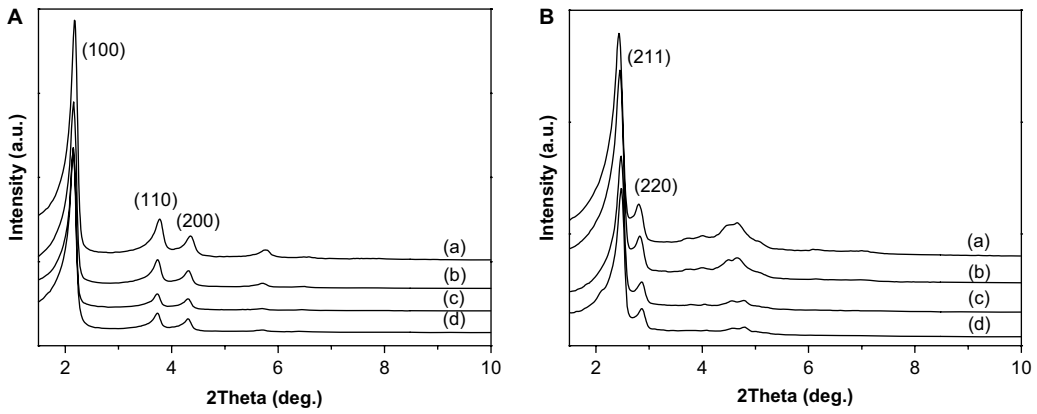

Figure 1. (A) Powder XRD patterns of (a) calcined 16MCM-41, (b) ME-16MCM-41, (c) **16M41-1**, and (d) **16M41-2**. (B) Powder XRD patterns of (a) calcined 16MCM-48, (b) ME-16MCM-48, (c) **16M48-1**, and (d) **16M48-2**.

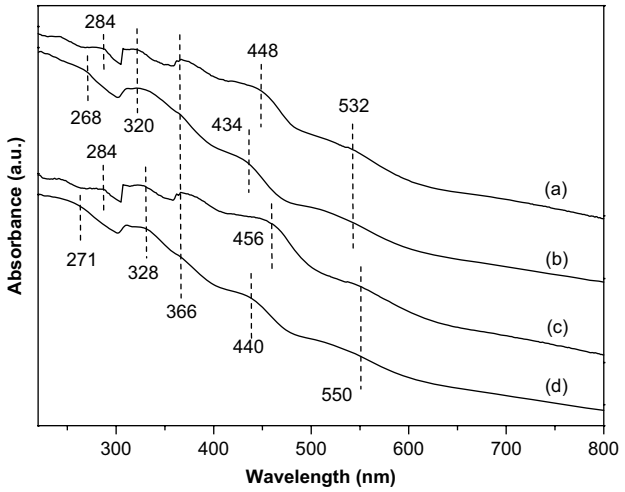

Figure 3. Diffuse-reflectance UV–vis spectra of (a) Mn(III) salen complex **1**, (b) the heterogeneous catalyst **16M48-1**, (c) Mn(III) salen complex **2**, and (d) the heterogeneous catalyst **16M48-2**.

The calcined mesoporous supports and the heterogeneous catalysts were characterized by N_2 sorption. Figure 4 shows the low-temperature N_2 adsorption–desorption isotherms and the pore size distributions of the heterogeneous catalysts **16M41-1**, **16M48-1**, **16M41-2**, and **16M48-2**. It can be seen that the immobilized catalysts maintained characteristic type IV isotherms[34] and uniform pore sizes in the mesopore ranges. The textural parameters of all the heterogeneous catalysts are presented in Table 2. Compared with parent supports (Table 1), a large decrease in BET surface area, pore volume, and pore diameter was observed on immobilization of chiral Mn(III) salen complexes onto mesoporous materials, which indicated that the active centers were located mainly on the inner surfaces of the supports.

3.3. The heterogeneous asymmetric epoxidation

The heterogeneous catalysts were evaluated in the epoxidation of styrene and indene in CH_2Cl_2 at 273 K for 8 h using *m*-CPBA/NMO as the oxidant. For comparison, the chiral Mn(III) salen catalysts **1** and **2** were also investigated under the same reaction conditions, but shortening the reaction time to 2 h. The effects of 3-mercaptopropyltrimethoxysilane dosage and the fine-tuning of pore size on the catalytic performance for the epoxidation of unfunctionalized olefins were studied.

3.3.1. Effect of 3-mercaptopropyltrimethoxysilane dosage on the catalytic performance

The chiral Mn(III) salen complexes were covalently anchored onto the surface of mesoporous materials through 3-mercaptopropyltrimethoxysilane. To investigate the effect of 3-mercaptopropyltrimethoxysilane dosage on the catalytic performance of heterogeneous catalysts, different amounts of 3-mercaptopropyltrimethoxysilane were immobilized on 16MCM-41 and 16MCM-48. The as-synthesized catalysts (e.g., **16M41-1** (*x* mL/g), where *x* denoted the amount of 3-mercaptopropyltrimethoxysilane used in the system containing 1.0 g of parent support) were evaluated in the asymmetric epoxidation of styrene. To effectively study the influence of 3-mercaptopropyltrimethoxysilane dosage, an excess of chiral Mn(III) salen complexes was used in the process of immobilization and the same amount of heterogeneous catalysts

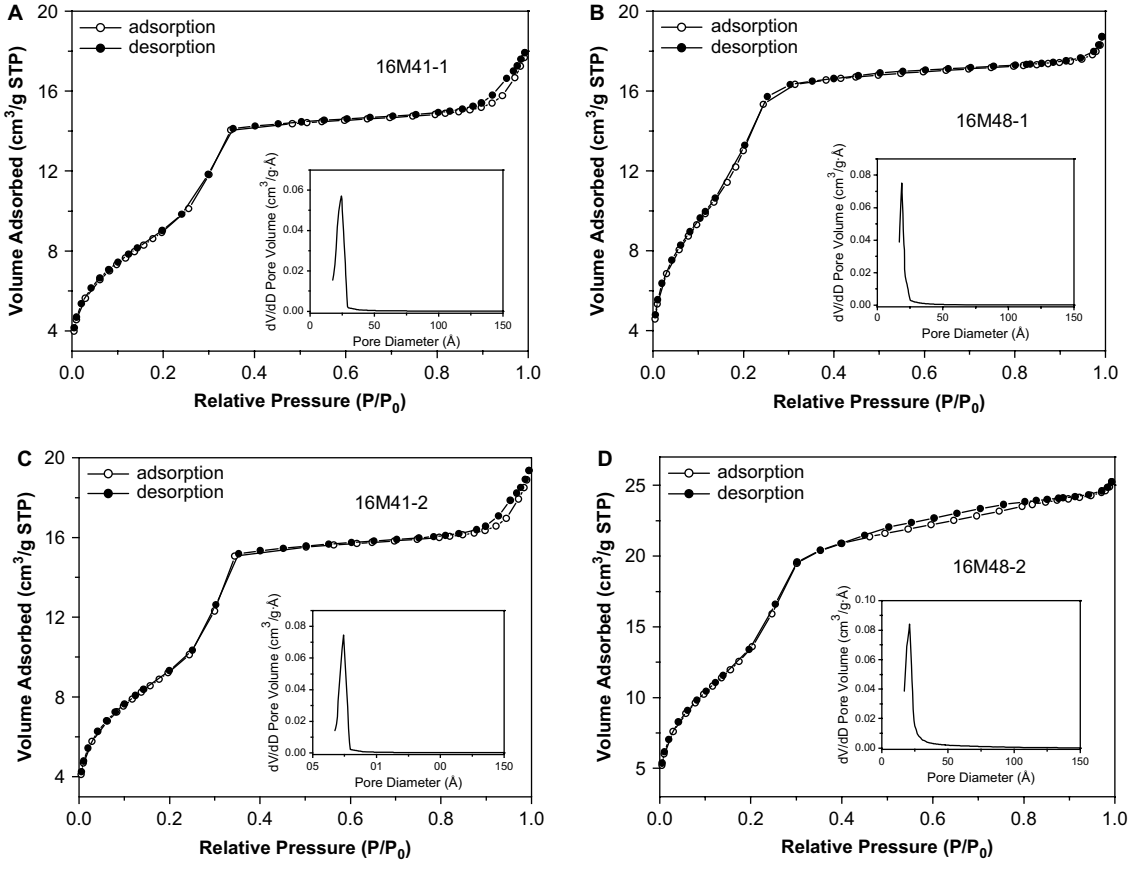

Figure 4. N_2 adsorption–desorption isotherms and pore diameter distribution profiles (inset) of (A) **16M41-1**, (B) **16M48-1**, (C) **16M41-2**, and (D) **16M48-2**.

Table 2
The structure parameters of heterogeneous catalysts

Sample	S_{BET} ($m^2\,g^{-1}$)	Pore volume ($cm^3\,g^{-1}$)	Pore diameter (Å)
18M41-1	755	0.62	27.0
16M41-1	744	0.58	24.4
14M41-1	779	0.51	19.1
12M41-1	769	0.50	17.3
16M48-1	1142	0.62	19.0
14M48-1	1083	0.46	18.9
12M48-1	1001	0.58	17.3
18M41-2	753	0.60	27.1
16M41-2	770	0.62	24.2
14M41-2	775	0.48	19.0
12M41-2	788	0.51	17.5
16M48-2	1154	0.85	21.1
14M48-2	1099	0.48	17.4
12M48-2	1055	0.57	17.0

(0.18 g, ca. 0.15 mol %) was employed in reaction system. Table 3 gives the results of styrene epoxidation catalyzed by the heterogeneous Mn(III) salen complexes that were anchored through different amounts of 3-mercaptopropyltrimethoxysilane onto the surfaces of 16MCM-41 and 16MCM-48. According to the results of elemental analysis, ca. 60% of 3-mercaptopropyltrimethoxysilane were linked on the surfaces of mesoporous supports.

As shown in Table 3, the dosage of 3-mercaptopropyltrimethoxysilane was related to the catalytic performance of heterogeneous catalysts. For the catalysts **16M41-1** and **16M48-1**, 0.4 mL of 3-mercaptopropyltrimethoxysilane was the most favorable to 1.0 g of parent supports. However, for the catalysts **16M41-2** and **16M48-2**, 0.2 mL of 3-mercaptopropyltrimethoxysilane to 1.0 g of parent supports was the best dosage. The high content of 3-mercaptopropyltrimethoxysilane would increase the diffusional resistance of chiral Mn(III) salen complexes into the channels and reactants to the active sites located on the inner surfaces of supports. On the other hand, low content of 3-mercaptopropyltrimethoxysilane would decrease the loading of chiral Mn(III) salen complexes and increase the leaching of active sites during the process of Soxhlet-extraction with dichloromethane. It could be seen from Table 3, the catalysts **16M41-2** and **16M48-2** obtained better catalytic performance at low dosage of 3-mercaptopropyltrimethoxysilane than the catalysts **16M41-1** and **16M48-1**. This is attributed mainly to the larger molecular size of complex **2**, which led to the higher diffusional resistance at high organic silane loading.

Table 3
Asymmetric epoxidation of styrene catalyzed by the immobilized chiral Mn(III) salen complexes anchored through different amounts of 3-mercaptopropyltrimethoxysilane[a]

Entry	Catalyst	Conv. (%)[b]	ee (%)[c]
1	**16M41-1** (0.2 mL/g)	51.7	17.3 (*R*)
2	**16M41-1** (0.4 mL/g)	62.4	20.9 (*R*)
3	**16M41-1** (0.6 mL/g)	59.4	19.0 (*R*)
4	**16M41-1** (1.0 mL/g)	57.6	16.6 (*R*)
5	**16M48-1** (0.2 mL/g)	62.1	26.1 (*R*)
6	**16M48-1** (0.4 mL/g)	69.3	29.6 (*R*)
7	**16M48-1** (0.6 mL/g)	58.1	18.0 (*R*)
8	**16M48-1** (1.0 mL/g)	44.0	15.4 (*R*)
9	**16M41-2** (0.1 mL/g)	58.4	25.7 (*R*)
10	**16M41-2** (0.2 mL/g)	64.7	25.7 (*R*)
11	**16M41-2** (0.4 mL/g)	61.3	23.7 (*R*)
12	**16M41-2** (0.6 mL/g)	58.9	22.2 (*R*)
13	**16M48-2** (0.1 mL/g)	72.3	40.1 (*R*)
14	**16M48-2** (0.2 mL/g)	76.9	41.2 (*R*)
15	**16M48-2** (0.4 mL/g)	73.2	39.0 (*R*)
16	**16M48-2** (0.6 mL/g)	58.1	22.7 (*R*)

[a] Reactions were performed in CH_2Cl_2 (10 mL) with catalyst (0.18 g, ca. 1.5 mol %), styrene (1 mmol), NMO (5 mmol), and *m*-CPBA (2 mmol) at 273 K for 8 h.
[b] Conversion % determined by GC with chiral column using toluene as internal standard.
[c] ee % determined by GC with RESTEK RT-BetaDEXse chiral column.

Table 4
Asymmetric epoxidation of styrene and indene catalyzed by the catalysts **1**, ***n*M41-1**, and ***n*M48-1**[a]

Entry	Catalyst	Substrate	Time (h)	Conv. (%) [b]	ee (%) [c]
1	**1**	Styrene	2	99.8	47.0 (*R*)
2	**18M41-1**		8	71.8	24.4 (*R*)
3	**16M41-1**		8	62.4	20.9 (*R*)
4	**14M41-1**		8	60.1	18.5 (*R*)
5	**12M41-1**		8	49.4	8.0 (*R*)
6	**16M48-1**		8	69.3	29.6 (*R*)
7	**14M48-1**		8	45.5	11.9 (*R*)
8	**12M48-1**		8	45.3	16.6 (*R*)
9	**1**	Indene	2	99.1	88.4 (1*R*,2*S*)
10	**18M41-1**		8	94.4	58.4 (1*R*,2*S*)
11	**16M41-1**		8	80.8	47.0 (1*R*,2*S*)
12	**14M41-1**		8	76.5	50.5 (1*R*,2*S*)
13	**12M41-1**		8	54.1	30.8 (1*R*,2*S*)
14	**16M48-1**		8	63.0	44.1 (1*R*,2*S*)
15	**14M48-1**		8	53.2	37.9 (1*R*,2*S*)
16	**12M48-1**		8	35.2	45.1 (1*R*,2*S*)

[a] Reactions were performed in CH_2Cl_2 (10 mL) with catalyst (0.015 mmol), substrate (1 mmol), NMO (5 mmol), and *m*-CPBA (2 mmol) at 273 K.
[b] Conversion % determined by GC with chiral column using toluene as internal standard.
[c] ee % determined by GC with RESTEK RT-BetaDEXse chiral column.

3.3.2. *Effect of the fine-tuning of pore size on the catalytic performance*

The heterogeneous catalysts supported by a series of mesoporous MCM-41 and MCM-48 materials with different pore sizes were evaluated in the epoxidation of styrene and indene, and the effect of the fine-tuning of pore size on their catalytic performance was studied. On the immobilization of chiral Mn(III) salen complexes **1** and **2**, the optimum 3-mercaptopropyltrimethoxysilane dosages were applied. The loading of complexes **1** and **2** in the heterogeneous catalysts was in the range of 0.07–0.08 mmol/g based on Mn element analysis by ICP-AES.

Table 4 gives the results of asymmetric epoxidation of styrene and indene catalyzed by the catalysts **1**, ***n*M41-1**, and ***n*M48-1**. In general, for the catalysts ***n*M41-1** and ***n*M48-1**, the catalytic activity increased with increasing the pore size. For instance, the highest conversions of styrene and indene were attained by the catalysts **18M41-1** and **16M48-1**, which possess the largest pore size. However, the enantioselectivity didn't run parallel to catalytic activity. The catalysts **18M41-1** and **16M48-1** exhibited the highest enantioselectivity

Table 5
Asymmetric epoxidation of styrene and indene catalyzed by the catalysts **2**, ***n*M41-2**, and ***n*M48-2**[a]

Entry	Catalyst	Substrate	Time (h)	Conv. (%) [b]	ee (%) [c]
1	**2**	Styrene	2	99.5	66.0 (*R*)
2	**18M41-2**		8	64.7	30.1 (*R*)
3	**16M41-2**		8	64.5	25.7 (*R*)
4	**14M41-2**		8	59.9	24.1 (*R*)
5	**12M41-2**		8	54.3	14.6 (*R*)
6	**16M48-2**		8	76.9	41.2 (*R*)
7	**14M48-2**		8	53.9	16.4 (*R*)
8	**12M48-2**		8	47.4	11.4 (*R*)
9	**2**	Indene	2	98.7	87.0 (1*R*,2*S*)
10	**18M41-2**		8	86.2	48.2 (1*R*,2*S*)
11	**16M41-2**		8	81.8	43.8 (1*R*,2*S*)
12	**14M41-2**		8	79.6	43.9 (1*R*,2*S*)
13	**12M41-2**		8	68.0	28.4 (1*R*,2*S*)
14	**16M48-2**		8	95.2	58.8 (1*R*,2*S*)
15	**14M48-2**		8	64.8	30.7 (1*R*,2*S*)
16	**12M48-2**		8	55.8	25.6 (1*R*,2*S*)

[a] Reactions were performed in CH_2Cl_2 (10 mL) with catalyst (0.015 mmol), substrate (1 mmol), NMO (5 mmol), and *m*-CPBA (2 mmol) at 273 K.
[b] Conversion % determined by GC with chiral column using toluene as internal standard.
[c] ee % determined by GC with RESTEK RT-BetaDEXse chiral column.

among the heterogeneous catalysts, but the catalyst **12M48-1** obtained higher ee values than **14M48-1** for the epoxidation of styrene and indene (entries 7, 8, 15, and 16) and the catalyst **14M41-1** presented better enantioselectivity than **16M41-1** for the epoxidation of indene (entries 11 and 12). This may be due to the confinement effect of the nanopores of 12MCM-48 and 14MCM-41, which were more compatible with the molecular size of styrene and indene.

Similarly, the catalysts **2**, ***n*M41-2** and ***n*M48-2** were also employed to catalyze the epoxidation of styrene and indene, and the results are listed in Table 5. It could be observed for the catalysts ***n*M41-2** and ***n*M48-2**, the immobilized catalysts based on the large-pore size mesoporous supports showed better activity and enantioselectivity, and the catalysts supported by the small pore size mesoporous materials exhibited lower conversions and ee values.

In summary, the catalytic performance of mesoporous materials supported catalysts was closely related to the pore sizes of the parent supports for the epoxidation of styrene and indene. The larger pore size of the supports would lead to higher conversions and ee values, however, the compatible pore size with substrate sometimes may be responsible for the improved ee values.

4. Conclusions

Two chiral Mn(III) salen complexes were synthesized from different chiral diamines and anchored through 3-mercaptopropyltrimethoxysilane onto a series of mesoporous materials with the pore sizes varied on the angstrom length-scale. The as-synthesized catalysts were characterized by XRD, FTIR, DR UV–vis, and N_2 sorption, and the results indicated that the chiral Mn(III) salen complexes were immobilized on the inner surface of the parent supports. The influence of 3-mercaptopropyltrimethoxysilane dosage on the catalytic performance of immobilized chiral Mn(III) salen catalysts was studied, and the optimum 3-mercaptopropyltrimethoxysilane dosage in the preparation of heterogeneous catalysts based on 16MCM-41 and 16MCM-48 was determined. Furthermore, the effect of the fine-tuning of pore size on the performance of heterogeneous catalysts was discussed. In general, the heterogeneous catalysts that immobilized onto the large-pore mesoporous supports exhibited higher activity, and the compatible pore size with substrate may be responsible for improved enantioselectivity in olefin epoxidation.

Acknowledgements

This work was supported by the National Natural Science Foundation of China (grant 20773069) and the National Key Technologies R&D Program of China (grant 2006BAC02A12).

References and notes

1. Zhang, W.; Loebach, J. L.; Wilson, S. R.; Jacobsen, E. N. *J. Am. Chem. Soc.* **1990**, *112*, 2801–2803.
2. Srinivasan, K.; Michaud, P.; Kochi, J. K. *J. Am. Chem. Soc.* **1986**, *108*, 2309–2320.
3. Zhang, H.; Li, C. *Tetrahedron* **2006**, *62*, 6640–6649.
4. Fache, F.; Schulz, E.; Tommasino, M. L.; Lemaire, M. *Chem. Rev.* **2000**, *100*, 2159–2232.
5. Song, C.-E.; Lee, S.-G. *Chem. Rev.* **2002**, *102*, 3495–3524.
6. Fan, Q.-H.; Li, Y.-M.; Chan, A. S. C. *Chem. Rev.* **2002**, *102*, 3385–3466.
7. Li, C. *Catal. Rev.—Sci. Eng.* **2004**, *46*, 419–492.
8. McMorn, P.; Hutchings, G. J. *Chem. Soc. Rev.* **2004**, *33*, 108–122.
9. Xia, Q.-H.; Ge, H.-Q.; Ye, C.-P.; Liu, Z.-M.; Su, K.-X. *Chem. Rev.* **2005**, *105*, 1603–1662.
10. Heitbaum, M.; Glorius, F.; Escher, I. *Angew. Chem., Int. Ed.* **2006**, *45*, 4732–4762.
11. Corma, A.; Garcia, H. *Adv. Synth. Catal.* **2006**, *348*, 1391–1412.
12. Baleizão, C.; Garcia, H. *Chem. Rev.* **2006**, *106*, 3987–4043.
13. Li, C.; Zhang, H.; Jiang, D.; Yang, Q. *Chem. Commun.* **2007**, 547–558.
14. Palucki, M.; Finney, N. S.; Pospisil, P. J.; Güler, M. L.; Ishida, T.; Jacobsen, E. N. *J.Am. Chem. Soc.* **1998**, *120*, 948–954.
15. Zhang, H.; Zhang, Y.; Li, C. *J. Catal.* **2006**, *238*, 369–381.
16. Kureshy, R. I.; Ahmad, I.; Khan, N. H.; Abdi, S. H. R.; Pathak, K.; Jasra, R. V. *Tetrahedron: Asymmetry* **2005**, *16*, 3562–3569.
17. Kureshy, R. I.; Ahmad, I.; Khan, N. H.; Abdi, S. H. R.; Pathak, K.; Jasra, R. V. *J. Catal.* **2006**, *238*, 134–141.
18. Lou, L.-L.; Yu, K.; Ding, F.; Zhou, W.; Peng, X.; Liu, S. *Tetrahedron Lett.* **2006**, *47*, 6513–6516.
19. Lou, L.-L.; Yu, K.; Ding, F.; Peng, X.; Dong, M.; Zhang, C.; Liu, S. *J. Catal.* **2007**, *249*, 102–110.
20. Kim, G.-J.; Shin, J.-H. *Tetrahedron Lett.* **1999**, *40*, 6827–6830.
21. Zhao, D.; Zhao, J.; Zhao, S.; Wang, W. *J. Inorg. Organomet. Polym.* **2007**, *17*, 653–659.
22. Yu, K.; Lou, L.-L.; Ding, F.; Wang, S.; Wang, Z.; Liu, S. *Catal. Commun.* **2006**, *7*, 170–172.
23. Yu, K.; Lou, L.-L.; Lai, C.; Wang, S.; Ding, F.; Liu, S. *Catal. Commun.* **2006**, *7*, 1057–1060.
24. Thomas, J. M.; Maschmeyer, T.; Johnson, B. F. G.; Shephard, D. S. *J. Mol. Catal. A: Chem.* **1999**, *141*, 139–144.
25. Raja, R.; Thomas, J. M.; Jones, M. D.; Johnson, B. F. G.; Vaughan, D. E. W. *J. Am. Chem. Soc.* **2003**, *125*, 14982–14983.
26. Larrow, J. F.; Jacobsen, E. N.; Gao, Y.; Hong, Y.; Nie, X.; Zepp, C. M. *J. Org. Chem.* **1994**, *59*, 1939–1942.
27. Zhang, H.; Xiang, S.; Xiao, J.; Li, C. *J. Mol. Catal. A: Chem.* **2005**, *238*, 175–184.
28. Kresge, C. T.; Leonowicz, M. E.; Roth, W. J.; Vartuli, J. C.; Beck, J. S. *Nature* **1992**, *359*, 710–712.
29. Beck, J. S.; Vartuli, J. C.; Roth, W. J.; Leonowicz, M. E.; Kresge, C. T.; Schmitt, K. D.; Chu, C. T.-W.; Olson, D. H.; Sheppard, E. W.; McCullen, S. B.; Higgins, J. B.; Schlenker, J. L. *J. Am. Chem. Soc.* **1992**, *114*, 10834–10843.
30. Yu, K.; Gu, Z.; Ji, R.; Lou, L.-L.; Ding, F.; Zhang, C.; Liu, S. *J. Catal.* **2007**, *252*, 312–320.
31. Minutolo, F.; Pini, D.; Petri, A.; Salvadori, P. *Tetrahedron: Asymmetry* **1996**, *7*, 2293–2302.
32. Casiraghi, G.; Casnati, G.; Cornia, M.; Pochini, A.; Puglia, G.; Sartori, G.; Ungaro, R. *J. Chem. Soc., Perkin Trans. 1* **1978**, 318–321.
33. Canali, L.; Cowan, E.; Deleuze, H.; Gibson, C. L.; Sherrington, D. C. *J. Chem. Soc., Perkin Trans. 1* **2000**, 2055–2066.
34. Sing, K. S. W.; Everett, D. H.; Haul, R. A. W.; Moscou, L.; Pierotti, R. A.; Rouquerol, J.; Siemieniewska, T. *Pure Appl. Chem.* **1985**, *57*, 603–619.